NASA/TM—2015-218758

NASA Glenn Icing Research Tunnel: 2014 and 2015 Cloud Calibration Procedures and Results

Laura E. Steen and Robert F. Ide
Sierra Lobo, Inc., Cleveland, Ohio

Judith F. Van Zante
Glenn Research Center, Cleveland, Ohio

Waldo J. Acosta
Jacobs Technology, Cleveland, Ohio

May 2015

NASA STI Program . . . in Profile

Since its founding, NASA has been dedicated to the advancement of aeronautics and space science. The NASA Scientific and Technical Information (STI) Program plays a key part in helping NASA maintain this important role.

The NASA STI Program operates under the auspices of the Agency Chief Information Officer. It collects, organizes, provides for archiving, and disseminates NASA's STI. The NASA STI Program provides access to the NASA Technical Report Server—Registered (NTRS Reg) and NASA Technical Report Server—Public (NTRS) thus providing one of the largest collections of aeronautical and space science STI in the world. Results are published in both non-NASA channels and by NASA in the NASA STI Report Series, which includes the following report types:

- TECHNICAL PUBLICATION. Reports of completed research or a major significant phase of research that present the results of NASA programs and include extensive data or theoretical analysis. Includes compilations of significant scientific and technical data and information deemed to be of continuing reference value. NASA counter-part of peer-reviewed formal professional papers, but has less stringent limitations on manuscript length and extent of graphic presentations.

- TECHNICAL MEMORANDUM. Scientific and technical findings that are preliminary or of specialized interest, e.g., "quick-release" reports, working papers, and bibliographies that contain minimal annotation. Does not contain extensive analysis.

- CONTRACTOR REPORT. Scientific and technical findings by NASA-sponsored contractors and grantees.

- CONFERENCE PUBLICATION. Collected papers from scientific and technical conferences, symposia, seminars, or other meetings sponsored or co-sponsored by NASA.

- SPECIAL PUBLICATION. Scientific, technical, or historical information from NASA programs, projects, and missions, often concerned with subjects having substantial public interest.

- TECHNICAL TRANSLATION. English-language translations of foreign scientific and technical material pertinent to NASA's mission.

For more information about the NASA STI program, see the following:

- Access the NASA STI program home page at http://www.sti.nasa.gov

- E-mail your question to help@sti.nasa.gov

- Fax your question to the NASA STI Information Desk at 757-864-6500

- Telephone the NASA STI Information Desk at 757-864-9658

- Write to:
  NASA STI Program
  Mail Stop 148
  NASA Langley Research Center
  Hampton, VA 23681-2199

NASA/TM—2015-218758

NASA Glenn Icing Research Tunnel: 2014 and 2015 Cloud Calibration Procedures and Results

Laura E. Steen and Robert F. Ide
Sierra Lobo, Inc., Cleveland, Ohio

Judith F. Van Zante
Glenn Research Center, Cleveland, Ohio

Waldo J. Acosta
Jacobs Technology, Cleveland, Ohio

National Aeronautics and
Space Administration

Glenn Research Center
Cleveland, Ohio 44135

May 2015

Acknowledgments

The authors would like to thank NASA's Aeronautics Test Program for funding this essential effort. Many thanks are also due to the other IRT Engineers: Seth Sederholm, Larry Becks, Mark Kubiak and Sean Currie; and the expert and very patient IRT Technicians: Joe August, Dave Bremenour, Jason Bryant, Paul Butterfield, Bill Magas, Rob Maibauer, Terry Mathes, Shaun McNea, Perry Vraja. Also thanks to Colin Bidwell, Dave Rigby, and Peter Struk for all their analysis and computing work to calculate the three-dimensional collection efficiencies on the multi-wire elements.

Level of Review: This material has been technically reviewed by technical management.

Available from

NASA STI Program
Mail Stop 148
NASA Langley Research Center
Hampton, VA 23681-2199

National Technical Information Service
5285 Port Royal Road
Springfield, VA 22161
703-605-6000

This report is available in electronic form at http://www.sti.nasa.gov/ and http://ntrs.nasa.gov/

NASA Glenn Icing Research Tunnel: 2014 and 2015 Cloud Calibration Procedures and Results

Laura E. Steen and Robert F. Ide
Sierra Lobo, Inc.
Cleveland, Ohio 44135

Judith F. Van Zante
National Aeronautics and Space Administration
Glenn Research Center
Cleveland, Ohio 44135

Waldo J. Acosta
Jacobs Technology
Cleveland, Ohio 44135

Abstract

This report summarizes the current status of the NASA Glenn Research Center (GRC) Icing Research Tunnel cloud calibration: specifically, the cloud uniformity, liquid water content, and drop-size calibration results from both the January–February 2014 full cloud calibration and the January 2015 interim cloud calibration. Some aspects of the cloud have remained the same as what was reported for the 2014 full calibration, including the cloud uniformity from the Standard nozzles, the drop-size equations for Standard and Mod1 nozzles, and the liquid water content for large-drop conditions. Overall, the tests performed in January 2015 showed good repeatability to 2014, but there is new information to report as well. There have been minor updates to the Mod1 cloud uniformity on the north side of the test section. Also, successful testing with the OAP-230Y has allowed the IRT to re-expand its operating envelopes for large-drop conditions to a maximum median volumetric diameter of 270 μm. Lastly, improvements to the collection-efficiency correction for the SEA multi-wire have resulted in new calibration equations for Standard- and Mod1-nozzle liquid water content.

Nomenclature

CDP	Cloud Droplet Probe, drop sizer, 2 to 50 μm
DeltaP	Spray nozzle Pwat–Pair (psid)
Dv0.##	drop diameter at which ##% of the total volume of water is contained in smaller drops
FZDZ	Freezing Drizzle
FZRA	Freezing Rain
LD	Large Drop conditions in the IRT: Mod1 nozzles, $2 \leq$ Pair ≤ 8 psig
LWC	Liquid Water Content (g/m^3)
MVD	Median Volumetric Diameter (μm)
OAP-230X	Optical Array Probe, drop sizer, 15 to 450 μm
OAP-230Y	Optical Array Probe, drop sizer, 50 to 1500 μm
Pair	Spray nozzle atomizing air pressure (psig)
Pwat	Spray nozzle water pressure (psig)

SLD	Supercooled large drops
TWC	Total Water Content (g/m^3)
V	Calibrated true air speed (velocity) in the test section (kn)

Introduction

SAE Aerospace Recommended Practices ARP5905, "Calibration and Acceptance of Icing Research Tunnels" (Ref. 1) requires that a full calibration be performed following any major facility upgrades. To comply with this, a full calibration was completed in January–February 2014, after the IRT replaced its Mod1 nozzles with newer versions that had tighter flow coefficients. The full results of that calibration are reported in Reference 2. In order to report the full current status of the IRT cloud, this report contains the results from that calibration that have not changed since 2014, which include Standard-nozzle cloud uniformity, Standard- and Mod1-nozzle drop-size equations, and large-drop liquid water content equations.

SAE ARP5905 (Ref. 1) also requires that an interim calibration be performed 1 yr following a full calibration to check the repeatability of the cloud uniformity, liquid water content and drop size calibrations. This interim calibration was completed January 5–9, 2015. IRT engineers ran abbreviated versions of the test matrices from the 2014 full calibration and compared the results to the previous data. These tests showed overall good repeatability to the 2014 tests, but there are also three updates to be reported. First, maintenance work was done on the spraybars in August 2014, and since that time there has been a high-low spot in the cloud uniformity, approximately 18 to 36 in. north of the test section centerline in the upper quadrant. Secondly, IRT engineers successfully ran an OAP-230Y probe, which allowed the IRT to reliably measure drop sizes larger than what could be measured in 2014. This resulted in a re-expansion of the previous operating envelopes, so that the maximum median volumetric diameter (MVD) in the IRT's calibrated operating range is now 270 μm. Lastly, NASA icing researchers have modified and improved the procedures used to calculate collection efficiency for the SEA multi-element sensor, and because of this the IRT has updated its liquid water content equations for Standard and Mod1 nozzles.

Calibration equations (transfer functions) are included in this report to relate the inputs of air speed, spray bar atomizing air pressure, and water pressure to the outputs of MVD and liquid water content (LWC). These correlations were completed for both 14 CFR Parts 25 and 29, Appendix C ('typical' icing) (Ref. 3) and Appendix O (supercooled large drop, or SLD) conditions (Ref. 4). The previous cloud calibration report (Ref. 2) summarizes the full results of the 2014 IRT full calibration, before the aforementioned updates were implemented. Many of the descriptions included in this 2015 report have been taken from that text where appropriate, including facility and hardware descriptions, common procedures, and descriptions of 2014 data.

Facility Description

The IRT is a closed-loop refrigerated wind tunnel that simulates flight through an icing cloud. A plan view of the facility is shown in Figure 1. A 5000 hp electric motor drives the 24 ft fan made of wood from Sitka spruce. The fan drives air through expanding turning vanes in "C-Corner," and into the face of the staggered heat exchanger. There, the air gets chilled/warmed within a temperature range of 20 °C total to –40 °C static. Twenty-four RTDs distributed on the D-Corner contracting turning vanes measure the total temperature in this D-Corner plenum area. The heat exchanger is 26 ft high and 50 ft wide.

Downstream of the D-Corner contracting turning vanes are 10 rows of spray bars with two different air-atomizing nozzle types: Mod1 (lower water flow rates) and Standard (higher water flow rates). Each bar has 55 nozzle positions that contain either a Mod1 nozzle, a Standard nozzle or a plug. Each nozzle location is fed from two water manifolds through remotely controlled solenoid valves. It is possible to

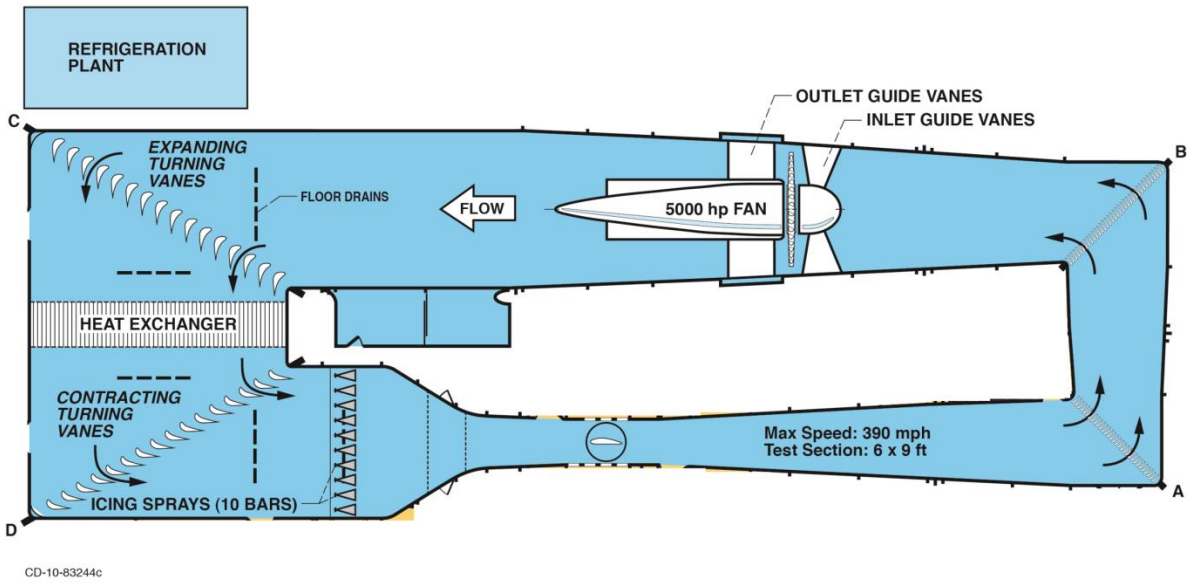

Figure 1.—A plan view schematic of the Icing Research Tunnel.

turn on only the Mod1 nozzles, only the Standard nozzles or both (with the same air pressure). The struts mounted vertically between spraybars that were required to help mix the cloud in 2006 are still required (Ref. 5).

The contraction area ratio into the test section is 14:1. The test section itself is 20 ft long (axial) by 6 ft high by 9 ft wide. The center of the test section is 44 ft from the spraybars. The calibrated speed range in the test section is from 50 to 325 kn. From the test section, the cloud flows into the diffuser toward A-Corner, and on around into B-Corner and into the fan.

Facility Change Notes

As described in Reference 2, the full cloud calibration that started in January 2014 followed the installation of new water tubes for the Mod1 nozzles. These new tubes were tested in-house and confirmed to have flow coefficients that varied by less than 3 percent of the average.

Additional maintenance work was done on the spray bars in August 2014. The solenoids and check valves were replaced at all active nozzle locations to address issues with the 17-year-old hardware. The solenoids open and close when a signal is sent to turn the spray nozzles on and off. The check valves ensure that no water leaks from one water manifold into the other, which could impact the manifold pressures.

Icing Cloud Uniformity

At the beginning of the 2014 full calibration, before the cloud characteristics of MVD and LWC could be determined, a uniform cloud was established. This was determined by identifying which of the 550 possible nozzle locations should spray Mod1, which should spray Standard nozzles, and which should be plugged. The 2014 process for creating a uniform cloud is explained in further depth in Reference 2.

Cloud uniformity was measured using a 6 by 6 ft grid. This grid extends floor to ceiling, and covers the central 6 ft of the 9 ft span. The grid mesh is 6 by 6 in. Mesh elements are 2 in. deep with a flat 1/8 in. face for ice accretion. Digital calipers were used to measure the ice thickness accreted at the center mesh points of the vertical elements. An image of a technician measuring ice on the grid is shown in Figure 2.

Figure 2.—A technician measures the thickness of ice accreted on the Grid.

For Standard nozzles, the cloud uniformity was very good in 2014, and it has been found to be very stable and repeatable over the past year. A representative Standard-nozzle cloud uniformity measured in 2015 is shown in Figure 3(a); the legend indicates a ratio of the local LWC measured on the grid compared to the average of the central twelve values. The light green color shows most of the map is within ±10 percent. The difference map is shown in Figure 3(b), which plots the differences between Figure 3(a) and what was measured for the same conditions in February 2014 (Figure 3 of Ref. 2), normalized by the average of the central 12 elements of the reference condition (Figure 3 of Ref. 2). These plots show there is excellent repeatability between the current Standard-nozzle uniformity map and the map from the Full Calibration in 2014, since nearly all differences are less than 10 percent.

The original Mod1 LWC uniformity results from 2014 are shown in Figure 4 for four airspeeds at an MVD of 20 μm. Similar, but not shown, are the uniformity plots as a function of MVD. These can be made available to customers upon request. Since the majority of the IRT's models are airfoils mounted vertically and centered in the test section, greater care was taken to make the spanwise central 12 to 12 in. as uniform as possible. Figure 4 shows that with a few exceptions, the uniformity is within ±10 percent.

After the maintenance work was done to the spraybars in August 2014, there has been a consistent high-low spot in the cloud uniformity on the north-center side of the test section, for Mod1 conditions only (including large-drop conditions, which use Mod1 nozzles). This can be seen in Figure 5, which shows the 150-kn Mod1 baseline that was measured in January 2015. Figure 5(a) is the measured cloud uniformity, plotted in the same way as Figure 3(a). Figure 5(b) shows the difference between this map and what was measured in February 2014 (Figure 4(b)), normalized by the average of the central 12 elements in the reference condition (Figure 4(b)). As can be seen from these figures, the non-uniform region is more than 18 in. off centerline, which is outside the typical customer testing region. Thorough investigations by the engineers and technicians did not uncover what caused this change in local cloud uniformity, but it has been consistent through tests conducted in August and September of 2014 and January 2015. This non-uniformity issue will be addressed as soon as schedule allows.

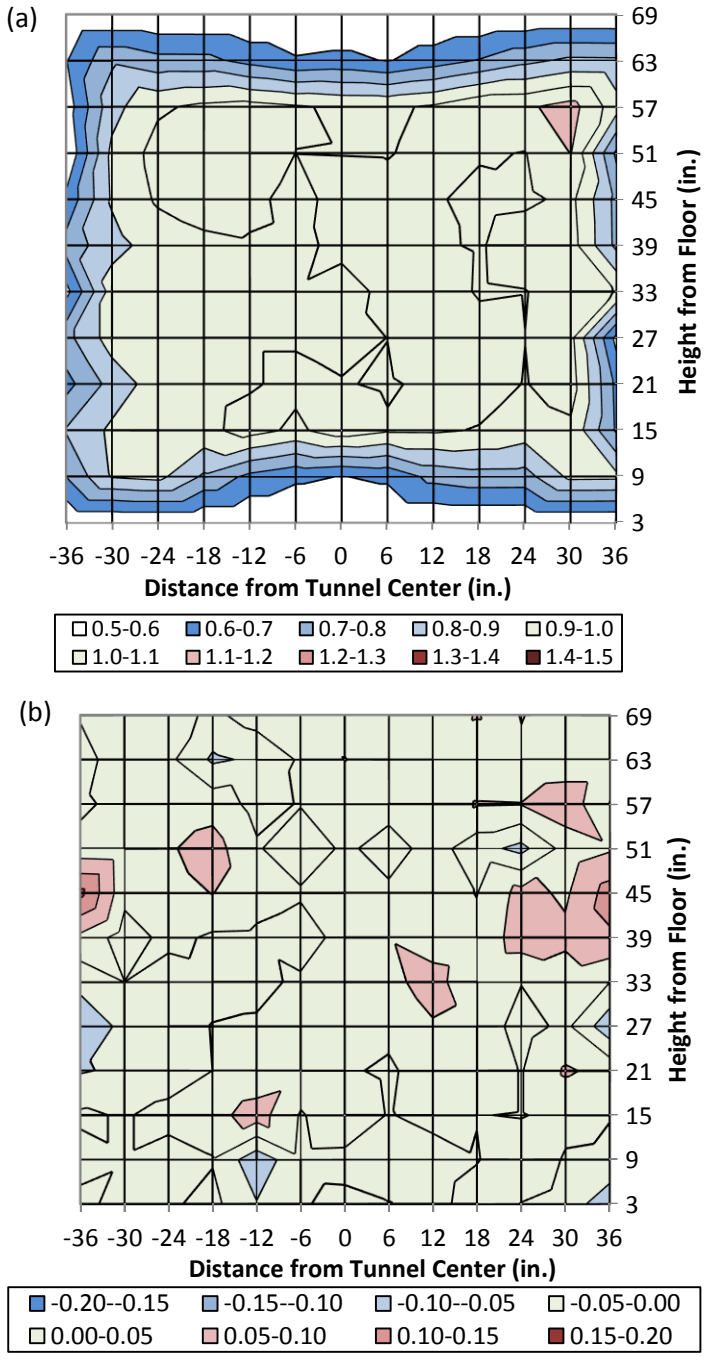

Figure 3.—Standard nozzle LWC uniformity for MVD = 20 μm, Pair = 20 psig, V = 150 kn, measured Jan. 2015. Note the two plots have different scales. (a) Ice thickness, plotted as a ratio of the average thickness of the central 12 elements. (b) Differences between Figure 3(a) (Jan. 2015) and Figure 3 of Ref. 2 (Feb. 2014), normalized by the average thickness of the central 12 elements from the Feb. 2014 measurement.

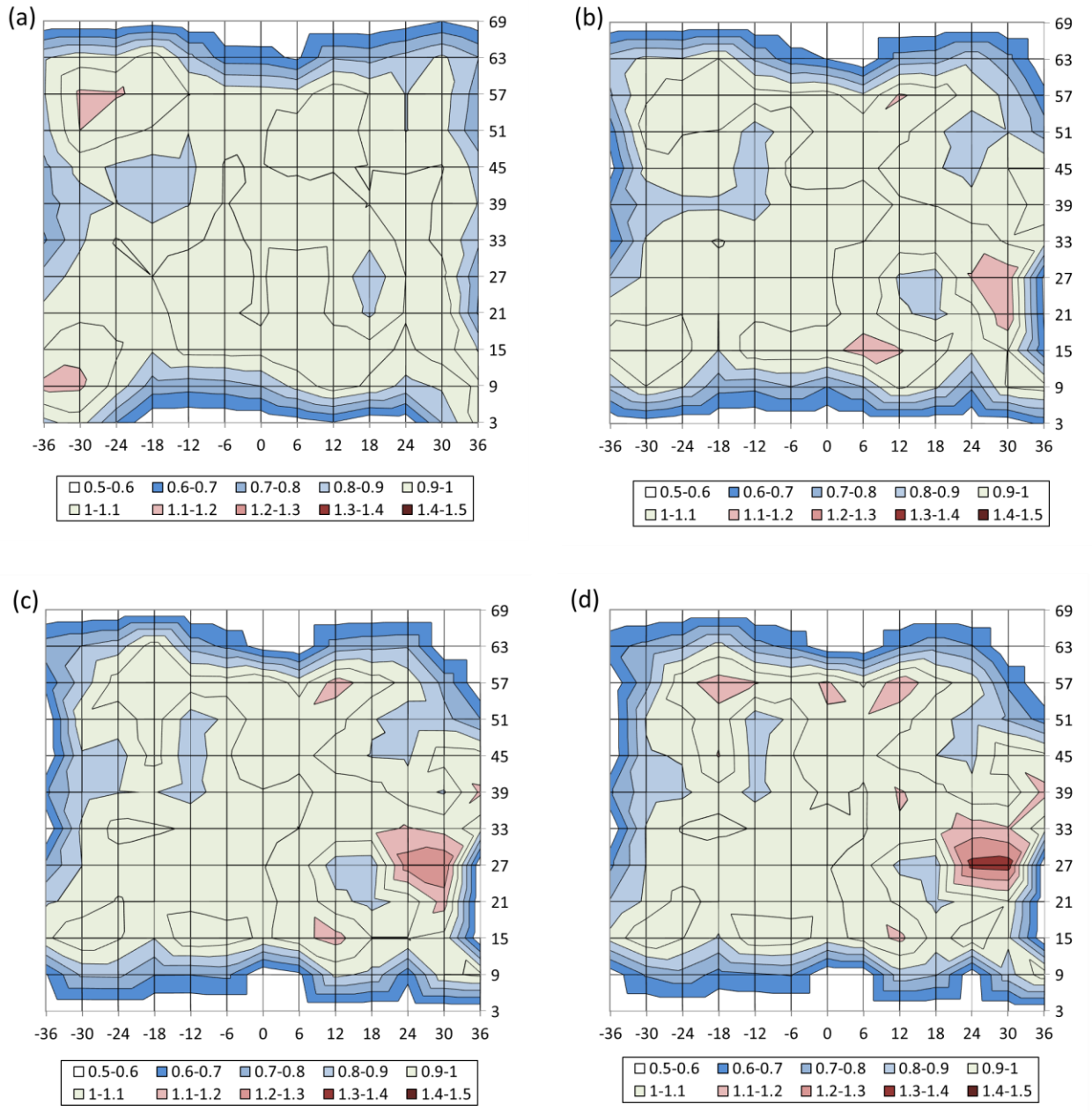

Figure 4.—Mod1 nozzle LWC uniformity plots measured in February 2014 at several airspeeds, MVD = 20 µm, Pair = 20 psig, V = (a) 100 kn, (b) 150 kn, (c) 200 kn, and (d) 250 kn. (Axes same as Figure 3). The values are plotted as a ratio of the average thickness of the central 12 elements.

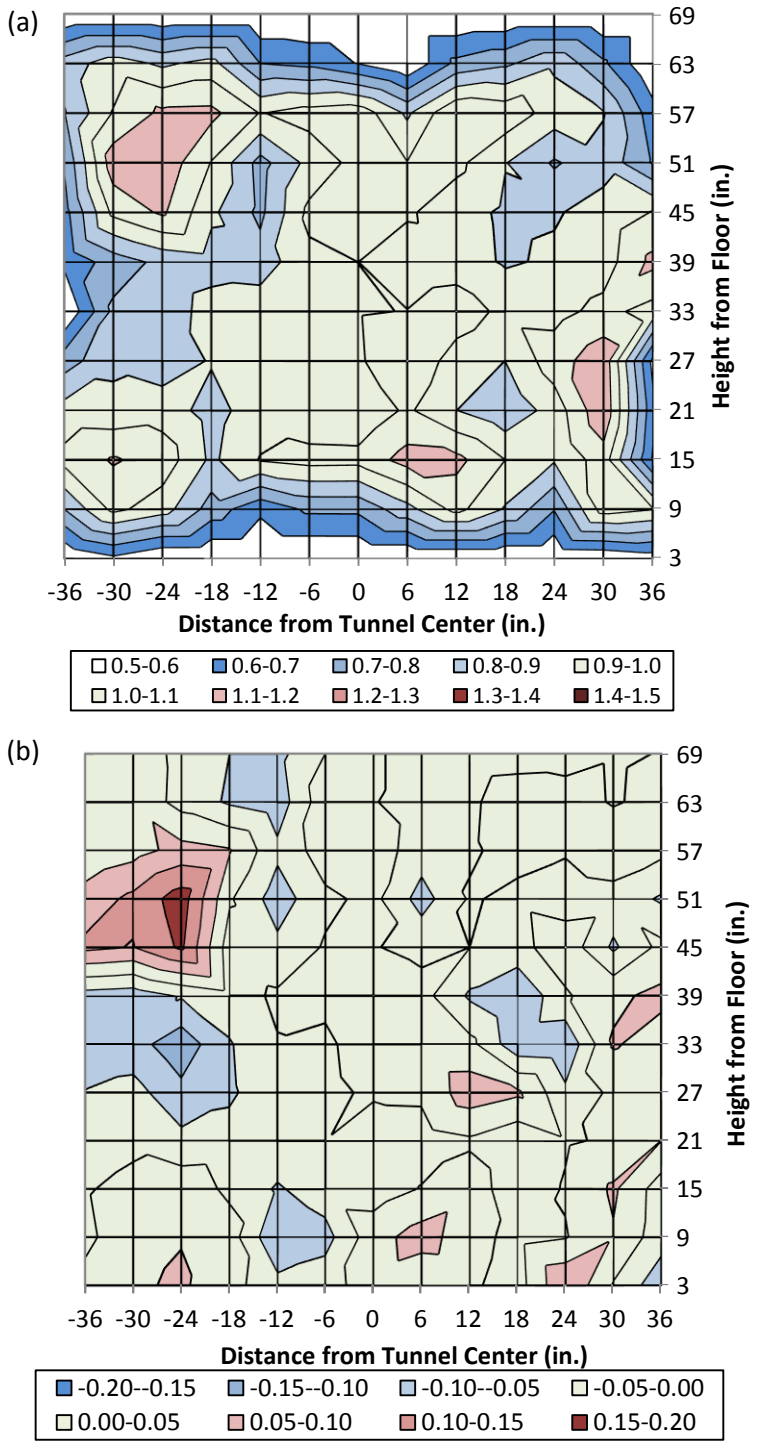

Figure 5.—Mod1 nozzle LWC uniformity plot for MVD = 20 µm, Pair = 20 psig, V = 150 kn, measured Jan. 2015. Note the two plots have different scales. (a) Ice thickness, plotted as a ratio of the average thickness of the central 12 elements. (b) Differences between Figure 5(a) (Jan. 2015) and Figure 4(b) (Feb. 2014) normalized by the average thickness of the central 12 elements from the Feb. 2014 measurement.

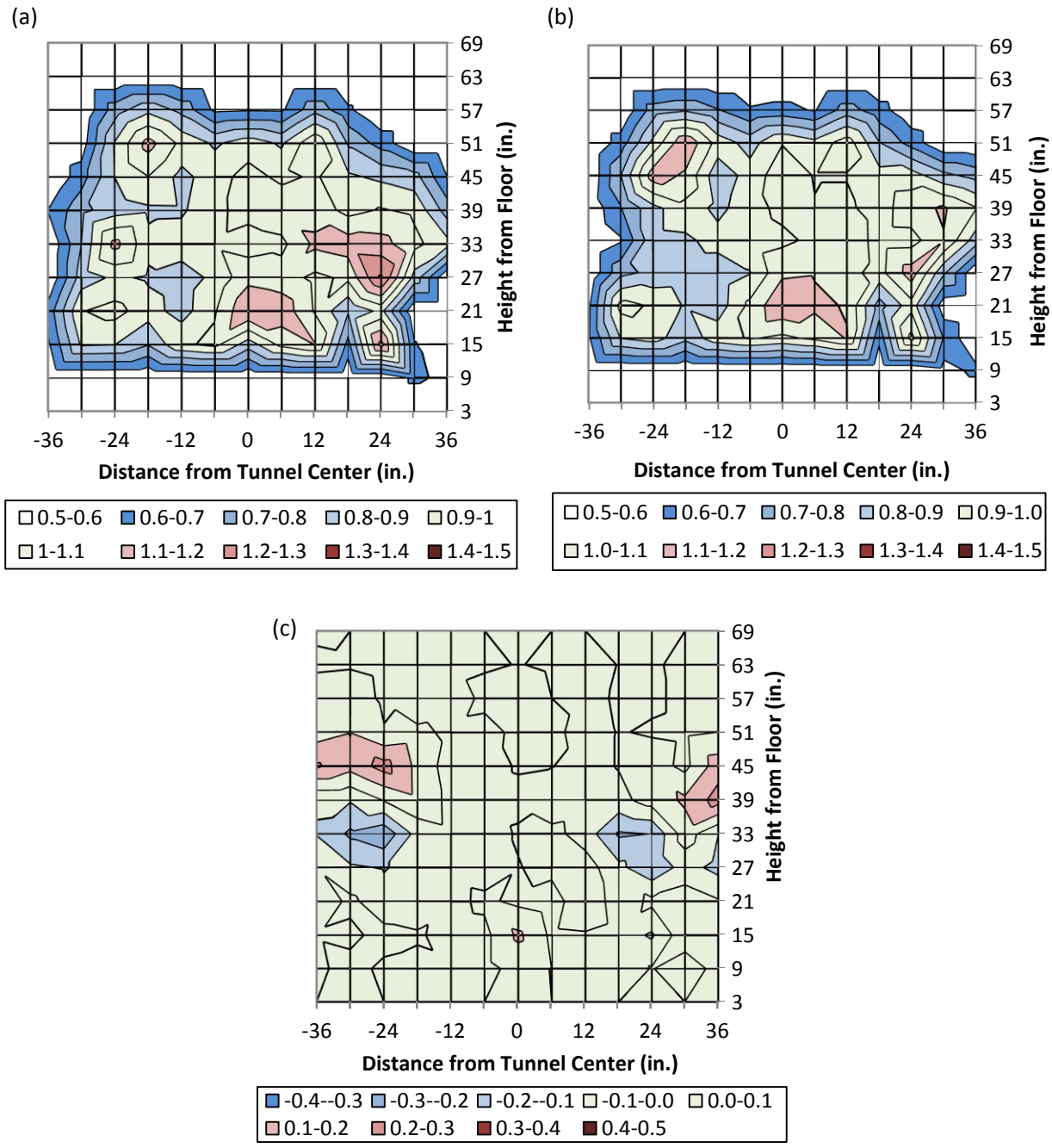

Figure 6.—LWC uniformity contour plot for a large-drop case, V = 150 kn, MVD = 100 µm, Pair = 3 psig, plotted as a ratio of the average thickness of the central 12 elements. (a) Ice thickness measured Feb. 2014. (b) Ice thickness measured Jan. 2015. (c) Differences between Figure 6(a) and Figure 6(b) (as a ratio of the central 12 elements in Figure 6(a)). Note that this plot has a different scale than the prior difference plots.

The cloud uniformity for a large-drop condition (MVD = 100 µm) measured in 2014 is shown in Figure 6(a). The vertical extent of the cloud is smaller than those in Figure 4, but the large drop uniformity is significantly improved over previous calibrations. The impact of the high-low spot, measured in January 2015, is shown in Figure 6(b). Figure 6(b) is the measured cloud uniformity, still plotted as a ratio of the average of the central 12 elements, and Figure 6c shows the differences between this map and what was measured in February 2014 (Figure 6(a)), normalized by the average of the central

12 elements in Figure 6(a). Again, the impact of the high-low spot is limited to the region more than 18 in. north of centerline. The scale for the difference plot has been changed from 5 to 10 percent because it gives a better representation of what might be expected from large-drop condition repeatability in the IRT.

Overall, the cloud uniformity results from the 2015 Interim Calibration showed good repeatability for the six conditions that were measured. In the vertical centerline region (±18 in. of the horizontal center of the test section) nearly all grid measurements matched the February 2014 measurements within 10 percent, for the Standard baseline, 150-kn Mod1 baseline, and large-drop baseline. Same-day repeatability measurements also showed less than 10 percent variation from what was measured at the start of the day.

Drop Size Calibration

Drop Size Data Acquisition

Data from three drop-sizing probes were used to build the 2014 and 2015 IRT drop-size calibration curves. These were the Cloud Droplet Probe, CDP (2 to 50 μm), Optical Array Probe, OAP-230X (15 to 450 μm), and OAP-230Y (50 to 1500 μm), which are shown in Figure 7. The CDP was made by Droplet Measurement Technologies, Inc. (Boulder, CO). The OAP-230X and OAP-230Y were made by the Particle Measurement Systems, Inc. and are no longer being manufactured. The IRT's OAP-230Y was not functional during the January 2014 tests, but it was repaired before the January 2015 tests.

The CDP measures drop sizes between 2 to 50 μm in diameter using the Mie-scattering theory for forward-scattered light intensity. Since the CDP measures the smallest drop sizes of the three probes and since all spray conditions in the IRT contain small drops, data from the CDP is collected and used for all spray conditions. Spray conditions ranged over the following: air pressures, Pair = 10 to 60 psig for the Standard nozzles and 2 to 60 psig for the Mod1 nozzles; delta pressures (water pressure minus air pressure), DeltaP = 5 to 150 psid for the Standard nozzles and 5 to 250 psid for the Mod1 nozzles. Both the OAP-230X and the OAP-230Y measure drop size using a shadowing technique. Data were taken with the OAP-230X for all spray conditions that produce a median volumetric diameter greater than approximately 18 μm. The OAP-230Y was only used for spray conditions that have historically produced a median volumetric diameter above 150 μm.

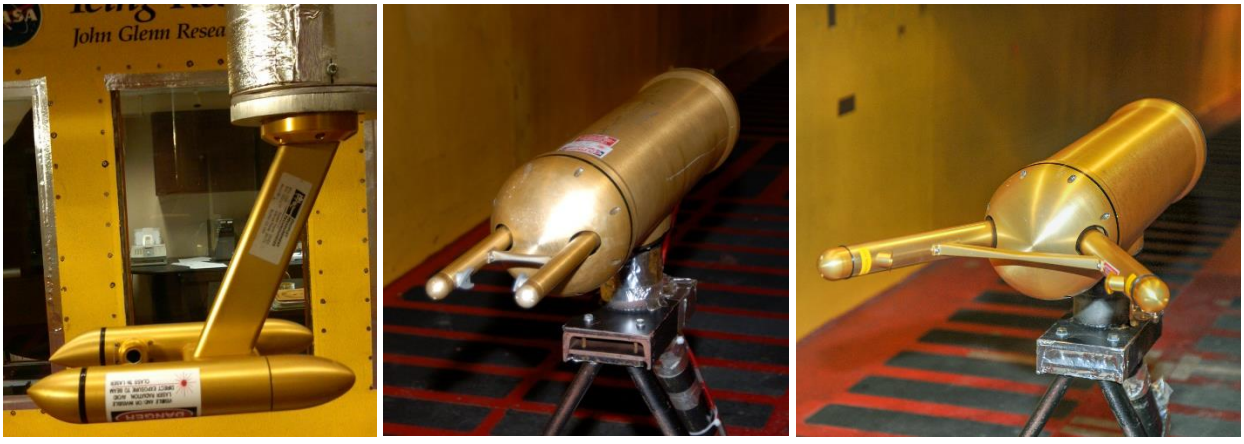

(a) (b) (c)

Figure 7.—Images of drop-sizing probes used for calibration in the IRT: (a) Cloud Droplet Probe (CDP), (b) Optical Array Probe (OAP-230X), (c) Optical Array Probe (OAP-230Y).

Data Processing of Drop Size Distributions

An example drop size distribution is shown in Figure 8, combining all three probes for a large-drop spray condition. The number density is the number of drops that are recorded in each bin normalized by its sample volume for that drop size and the bin width. The squares show the size distribution as measured by the CDP, the triangles show the size distribution as measured by the OAP-230X, and the circles show the size distribution as measured by the OAP-230Y. Note that the first three bins of the OAP-230X (the smaller black triangles) overlap with the CDP, and the first 9 bins of the OAP-230Y (the smaller black circles) overlap with the OAP-230X; these bins are not used in the drop size calculation.

The median volumetric diameter (MVD) is used to characterize the drop size distribution. This is the value at which half of the water volume is contained in smaller (or larger) drops; MVD is also referred to as Dv0.5. Correspondingly, Dv0.9 is the diameter at which 90 percent of the volume is contained in smaller drops. Normalized cumulative volume distributions for the IRT are shown in Figure 9. Bin volumes are plotted cumulatively, such that each data point represents the amount of water contained in all smaller diameters, normalized by the total volume contained in all bins. Figure 9(a) shows cumulative volume distributions for MVD values less than or equal to 50 µm and Figure 9(b) shows cumulative volume distributions for MVD values greater than 50 µm.

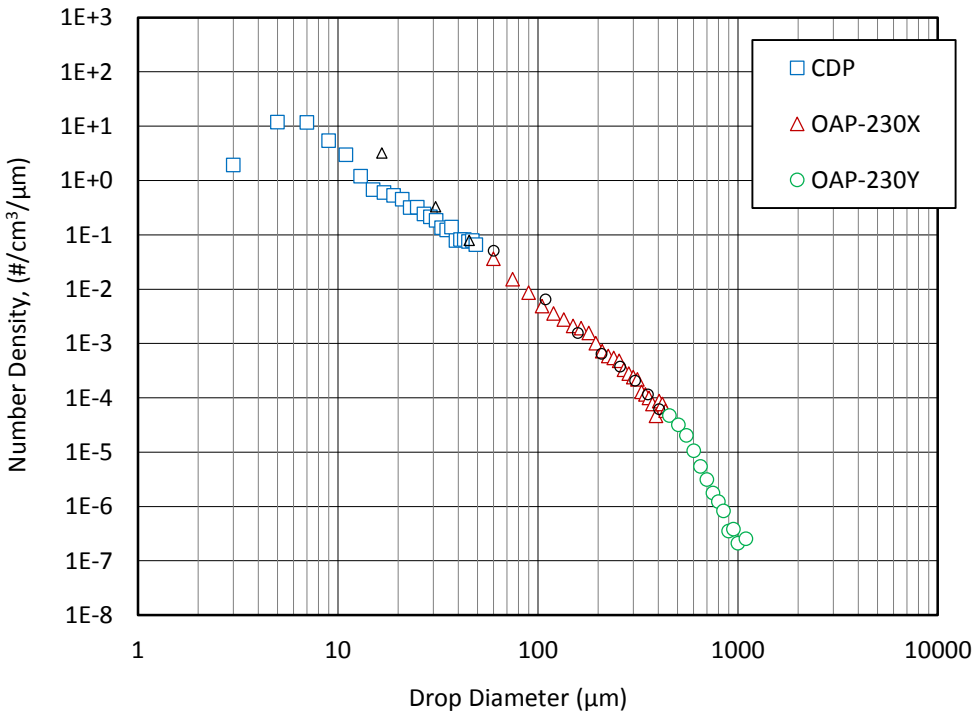

Figure 8.—Drop size distribution presented as number density versus drop diameter, measured by the CDP + OAP-230X + OAP-230Y, MVD = 270 µm. The smaller, black triangles and circles are overlap points and are not used in MVD calculations.

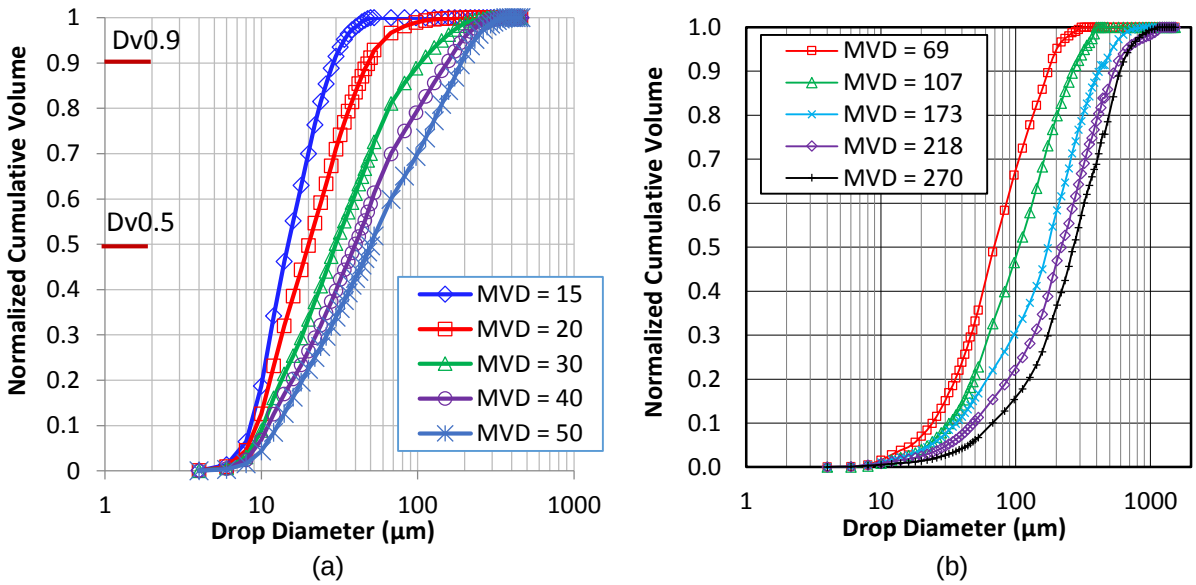

Figure 9.—Normalized cumulative volume distributions: (a) MVD ≤ 50 µm with Dv0.5 (= MVD) and Dv0.9 indicated, (b) MVD > 50 µm.

Drop Size Equations

The MVD curve fit equations were determined by inputting the measured Pair, DeltaP and MVD from the January 2014 tests into the curve fit generator TableCurve (Systat Software, Inc.). The equations that were generated, while quite complex, fit the majority of the data within 10 percent, which is the typical target for the IRT. Different curve fits were generated for the Standard and Mod1 nozzles.

The Standard MVD curve fit equation is,

$$MVD_{Standard} = \frac{a+b*(Pair)+c*(Pair)^2+d*\ln(DeltaP)}{1+e*(Pair)+f*(Pair)^2+g*(Pair)^3+h*\ln(DeltaP)} \quad (1)$$

where a = 19.034, b = 0.0927, c = 0.00150, d = -3.945, e = 0.0474, f = -0.000669, g = 0.00000497, h = -0.438.

The Mod1 MVD curve fit equation is

$$MVD_{Mod1} = a + b*(Pair)^c + d*(DeltaP)^e + f*(Pair)^c*(DeltaP)^e \quad (2)$$

where a = 12.178, b = 267.014, c = -2.184, d = 0.00112, e = 1.362, f = 22.742.

Figure 10 and Figure 11 summarize these MVD curve fits for Standard and Mod1 nozzles, respectively, and include data from both January 2014 and January 2015. In Figure 10(a) and Figure 11(a), the curve fit lines are plotted as a function of DeltaP for each calibrated Pair line. Measured MVDs are plotted against the respective curve fits for two Pair lines in each plot. Figure 10(b) and Figure 11(b) show how the curve fit values from the above equations compare to the measured values for all Standard and Mod1 conditions. The 1:1 line, as well as ±10 percent lines are shown for reference. These plots show that the curve fits for the vast majority of the data points are within the IRT's typical targeted accuracy of 10 percent. These plots also show that the MVD values measured in 2015 still fit within 10 percent of the curve fit. Thus, no changes to the calibration curves were necessary for normal Standard- and Mod1-nozzle operating conditions.

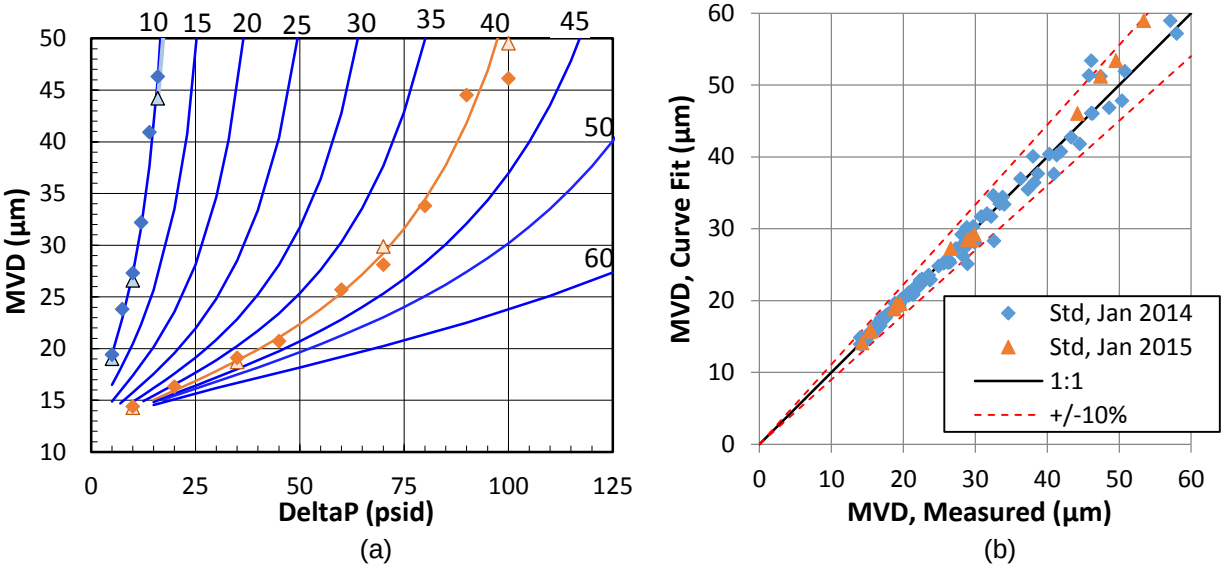

Figure 10.—Drop size calibration curves for the Standard Nozzles: (a) MVD versus DeltaP for each (labeled) Pair line. The curves are the fit. The measured MVD for Pair = 10 and 40 psig lines are also plotted as data points. The diamonds were measured in January 2014 and the triangles were measured in January 2015. (b) Curve fit versus measured MVD for all Standard-nozzle calibration points, including both January 2014 and January 2015.

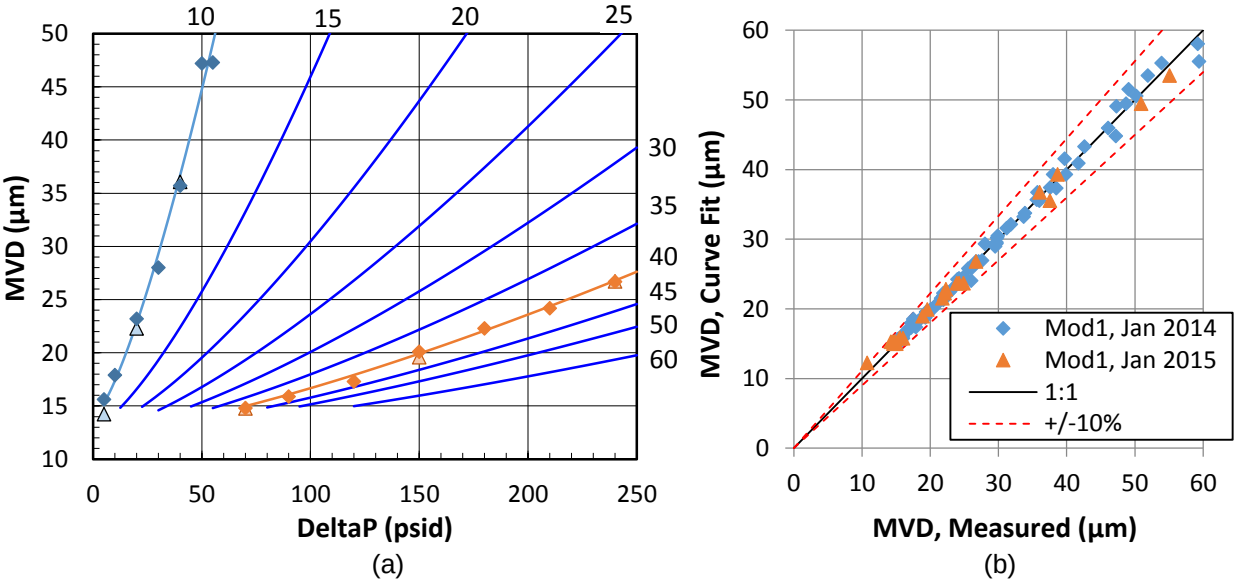

Figure 11.—Drop size calibration curves for the Mod1 Nozzles: (a) MVD versus DeltaP for each (labeled) Pair line. The curves are the fit. The measured MVD for Pair = 10 and 40 psig lines are also plotted as data points. The diamonds were measured in January 2014 and the triangles were measured in January 2015. (b) Curve fit versus measured MVD for all Mod1-nozzle calibration points, including both January 2014 and January 2015.

Large-Drop Conditions in the IRT

A significant, current question is the IRT's ability to produce supercooled large drops or SLD. Larger drops are achievable by reducing the spray nozzle atomizing air pressures so there is less breakup of the water stream. Operating the Mod1 nozzles between $2 \leq \text{Pair} \leq 8$ psig is referred to as "large-drop conditions" in the IRT. This is merely a short-hand phrase to identify this calibration regime.

The January 2015 tests with the OAP-230Y were successful, which allowed the IRT to reliably measure drop sizes larger than what could be measured in 2014. In 2014, the maximum calibrated MVD was 175 µm due to difficulties with the large-dropsize probes (Ref. 2). The largest calibrated MVD is now 270 µm. The new 2015 calibration curves for the large-drop conditions were created using data from both January 2014 (CDP + OAP-230X) and January 2015 (CDP + OAP-230X + OAP-230Y). The measured Pair, DeltaP and MVD values were put into the curve fit generator TableCurve (Systat Software, Inc.). The MVD curve fit equation for large-drop conditions is,

$$MVD_{LD} = a + b * \ln(Pair) + c * (DeltaP)^2 + d * (\ln(Pair))^2 + e * (DeltaP)^2 + f * DeltaP * \ln(Pair) + g * (\ln(Pair))^3 + h * (DeltaP)^3 + i * (DeltaP)^2 * \ln(Pair) + j * DeltaP * (\ln(Pair))^2$$

Where a = 124.311, b = –149.332, c = 12.966, d = 25.254, e = –0.0678, f = –5.492, g = 15.519, h = –0.0012, i = 0.106, and j = –1.383. Figure 12 shows the new calibration curves as well as the comparison between all measured values and the curve fit. The curves shown in Figure 12(a) have been plotted to show the bounds of the IRT's calibrated range for MVDs in large-drop conditions. Fitting both the 2014 and 2015 data sets led to a less than optimal curve fit trend. Bounds on the pressure lines are required to keep the fits realistic. Nevertheless, Figure 12(b) shows the fit is accurate to within ±20 percent, which is a historically typical accuracy for the IRT in large-drop conditions.

Comparisons of the IRT distributions to the FAA Appendix O (Ref. 4) requirements are shown in Figure 13 for both Freezing Drizzle (FZDZ) and Freezing Rain (FZRA) conditions. For FZDZ, MVD < 40 µm (Figure 13(a)) and FZDZ, MVD > 40 µm (Figure 13(b)), IRT distributions are selected that match the MVD (Dv0.5), or Dv0.98. Matching Dv0.98 (or similarly, Dv0.95 or 0.90) rather than the MVD would better assure that the effects of the larger drops in the distribution are captured. Also recognize that FZDZ, MVD < 40 µm conditions can be met with the more normal operation of Pair > 10 psig for the Mod1 nozzles. This is due to the fact that the IRT nozzles have long "tails"; that is, the largest drops produced for a spray condition are typically three to six times the MVD value.

Figure 13(c) plots the same data as Figure 8, except in the form of a normalized cumulative volume distribution. The IRT data that are plotted in Figure 8 and Figure 13(c) represent the maximum MVD in the IRT's calibrated operating range. For reference, Figure 13(c) compares this dropsize distribution to the FAA's two freezing rain (FZRA) distributions, MVD < 40 µm and MVD > 40 µm (Ref. 4).

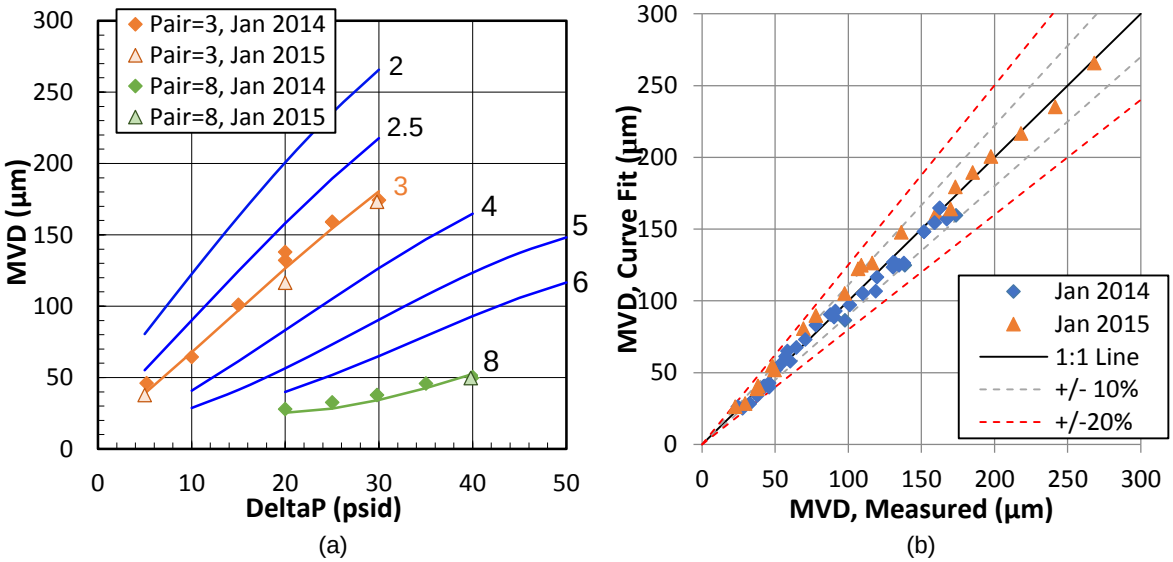

Figure 12.—Drop size calibration curves for large-drop conditions: (a) MVD versus DeltaP for each (labeled) Pair line. The curves are the fit. The measured MVD for Pair = 3 and Pair = 8 psig are also plotted as data points. (b) Curve fit versus measured MVD for all measured large-drop conditions.

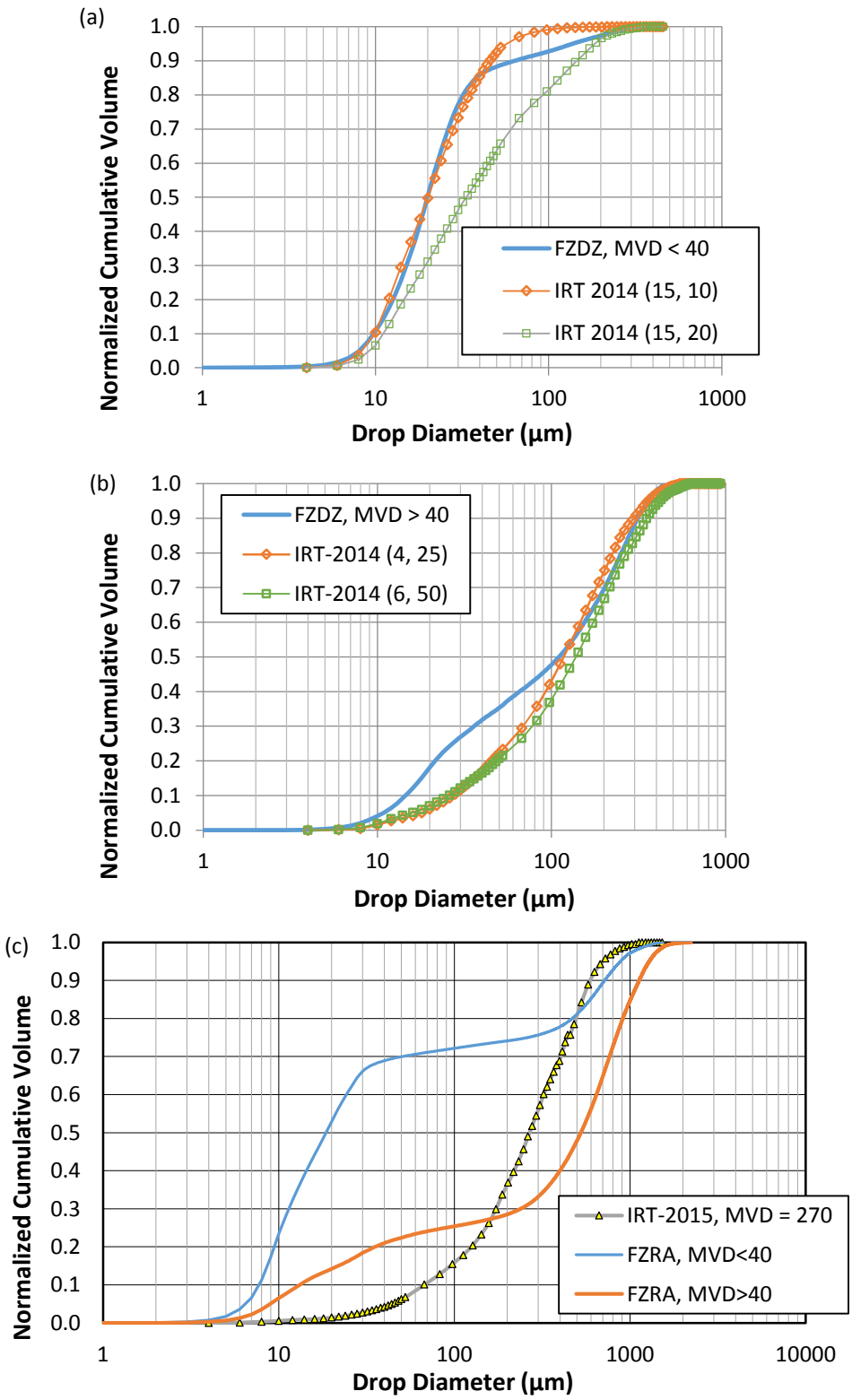

Figure 13.—Comparison of IRT distributions to FAA Appendix O conditions (Ref. 4) for (a) FZDZ, MVD < 40 µm, (b) FZDZ, MVD > 40 µm, (c) FZRA, MVD < 40 µm and MVD > 40 µm, plotted against the drop size distribution for the largest MVD in the IRT's calibrated range.

Another concern with producing large drops in any facility is the ability to supercool them. A numerical and experimental study was conducted for and in the IRT (Ref. 6). Though the number of cases was limited, it found that 160 μm MVD drops (max. drop size approximately 400 μm) at V = 195 mph were 1.9 °F warmer than the static air temperature in the test section. As drop size increases, it can be expected that the difference between the drop temperature and the static air temperature will increase.

Liquid Water Content

Liquid Water Content Data Acquisition

A multi-wire instrument manufactured by Science Engineering Associates (SEA; Mansfield Hollow, CT) was used to generate the liquid water content (LWC) calibration. A picture of this instrument is shown in Figure 14. There are four elements within the anti-iced probe head. The three vertical elements (perpendicular to the flow) are a 0.5 mm wire, 2-mm-cylindrical tube, and a 2-mm-half-pipe element. The wire and cylindrical tube primarily measure LWC while the half pipe captures both LWC and ice particles (if present). The half-pipe measurement is therefore called total water content (TWC); it is the primary sensor used in the IRT for LWC measurements. The fourth element is a compensation wire which is placed behind the center element and parallel to the flow. It is designed to stay dry so that it tracks air temperature, air pressure and airspeed effects only. The four heated elements are held at a constant temperature of 140 °C. The power required to maintain this temperature is proportional to the amount of water each element must evaporate. SEA defines the LWC calculation as (Ref. 7):

$$LWC\ \left(\frac{g}{m^3}\right) = \frac{C * P_{sense,wet}}{\left[L_{evap} + (T_{evap} - T_{amb})\right] * V * L_{sense} * W_{sense}} \quad (4)$$

where $C = 2.389*10^5$, $P_{sense,wet} = P_{sense,total} - P_{comp}$ = wet power (W) measured by the sense element, L_{evap} = latent heat of evaporation (cal/g), T_{evap} = evaporative temperature (C), T_{amb} = ambient static temperature (C), L_{sense} and W_{sense} = length and width respectively of the sense element (mm) and V = true airspeed (m/s). $P_{sense,total}$ is the total power measured by the element, P_{comp} is the power measured by the compensation element.

Figure 14.—The Multi-wire liquid water content instrument mounted in the icing tunnel.

2015 Update in Collection Efficiency Correction

In 2015, there was an update in the LWC calibration curves for Standard- and Mod1-nozzles due to a change in data processing. The same multi-element sensor head was used for the liquid water content (LWC) portion of the 2015 Interim Calibration as was used for the full calibration in 2014, and the raw results repeat the January 2014 measurements within tolerance (±10 percent). However, the collection-efficiency correction values that are used for post-processing the data have been improved. The previous collection-efficiency values were calculated by the FWG two-dimensional particle trajectory code, (Ref. 8), which uses an isolated, infinite element. Recent work by Rigby, Struk, and Bidwell (Ref. 9) improved these calculations by performing a three-dimensional analysis of the fluid flow and the corresponding spherical particle trajectories around the total-water content sensor, also modeling the impacts of the shroud and the two other sensing elements. Rigby et al. found that the collection-efficiency values decreased, particularly for smaller drops and lower airspeeds. Struk then conducted additional analysis (Ref. 10) to apply these calculations to particle-size distributions rather than just the MVD measured in the IRT. Based on this work, the IRT has developed new three-dimensional values for collection efficiency that are now being used in post-processing multi-element sensor data.

When the new three-dimensional collection efficiencies were applied to the 2014 Full Calibration multi-wire measurements for Standard- and Mod1-nozzle conditions, the LWC values were about 5 percent higher than they were with the two-dimensional collection efficiency correction, as shown in Figure 15. The differences were large enough to warrant an adjustment to the LWC calibration curves.

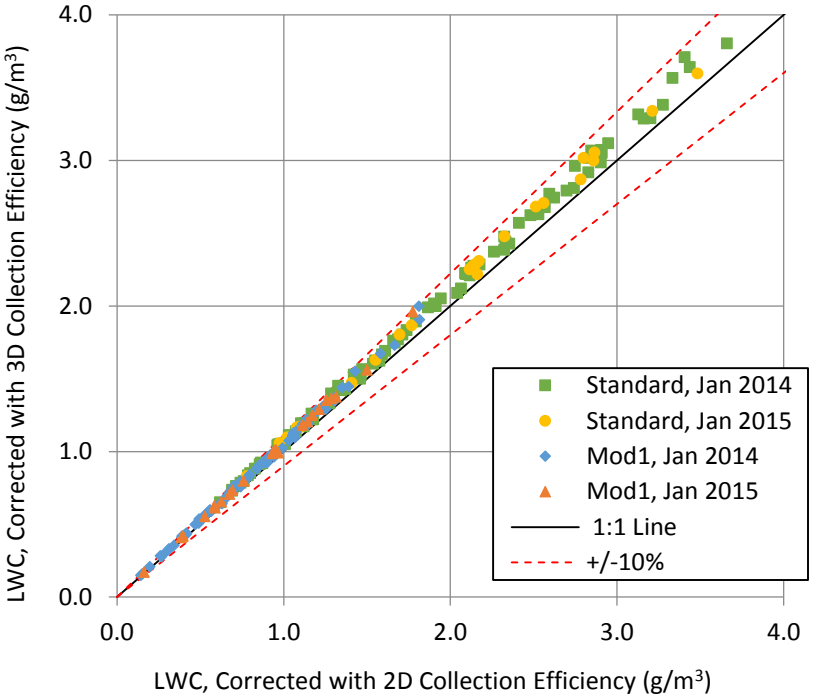

Figure 15.—Comparison of total-water-content data, corrected with three-dimensional collection efficiency versus two-dimensional collection efficiency, using Mod1- and Standard-nozzle data from January 2014 and January 2015.

Liquid Water Content Equations

The new LWC calibration curves for normal Standard- and Mod1-nozzle conditions were developed from the January 2014 data, corrected with the new three-dimensional collection efficiency. The equations correlate liquid water content to Pair, DeltaP, and test section airspeed (V). As described in the 2006 IRT calibration report (Ref. 5), the liquid water content calibration is a function of the form:

$$LWC = K(V, Pair) * \frac{\sqrt{DeltaP}}{V} \tag{5}$$

where K is a function of velocity and Pair. The first step of fitting the LWC curve is to determine the function K for both parameters, "Kv" and "Ka". To do this, measurements were made from V = 50 to 325 kn while Pair and DeltaP (and MVD) are held constant, defining Kv. Ka is defined by holding velocity and MVD constant while making measurements from Pair = 10 to 60 psig. K is calculated for each of these measured values based on the above relationship: $K = LWC * V/\sqrt{DeltaP}$. Figure 16 shows the linear relationships found when K was correlated to velocity and Pair for both Mod1 and Standard nozzles. These linear fits are combined to determine the planar function K. An additional correction factor was added after it became apparent that even with this curve fit optimized, there was a clear correlation of LWC to MVD for both the Mod1 and Standard nozzle sets. From this, the 2015 Standard LWC equation is as follows:

$$LWC_{Standard} = (a * V + b * Pair + c) * \left(\frac{MVD - 3}{d}\right)^{e} * \frac{\sqrt{DeltaP - 1}}{V}$$

where a is the slope of the Kv versus V line, b is the slope of the Ka versus Pair line, d is a basis MVD and c and e are constants. For this equation, a = 0.1564, b = –0.3119, c = 47.6, d = 20, and e = 0.12. Additional correction factors were added to the MVD and DeltaP terms to improve the fit. For the Standard nozzles, the curve fit predicts the vast majority of the measured values within ±10 percent, as shown in Figure 17(a), comparing both the January 2014 and the January 2015 data.

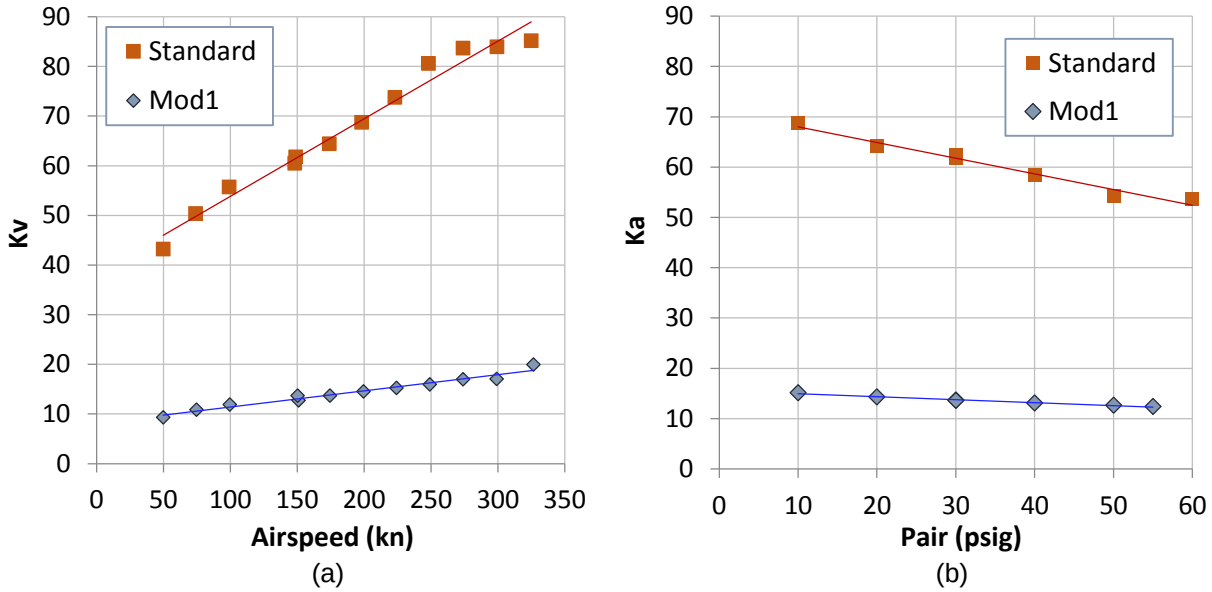

Figure 16.—LWC parameters, K, for the Standard and Mod1 nozzles sets showing the effect of (a) Kv versus airspeed, and (b) Ka versus Pair.

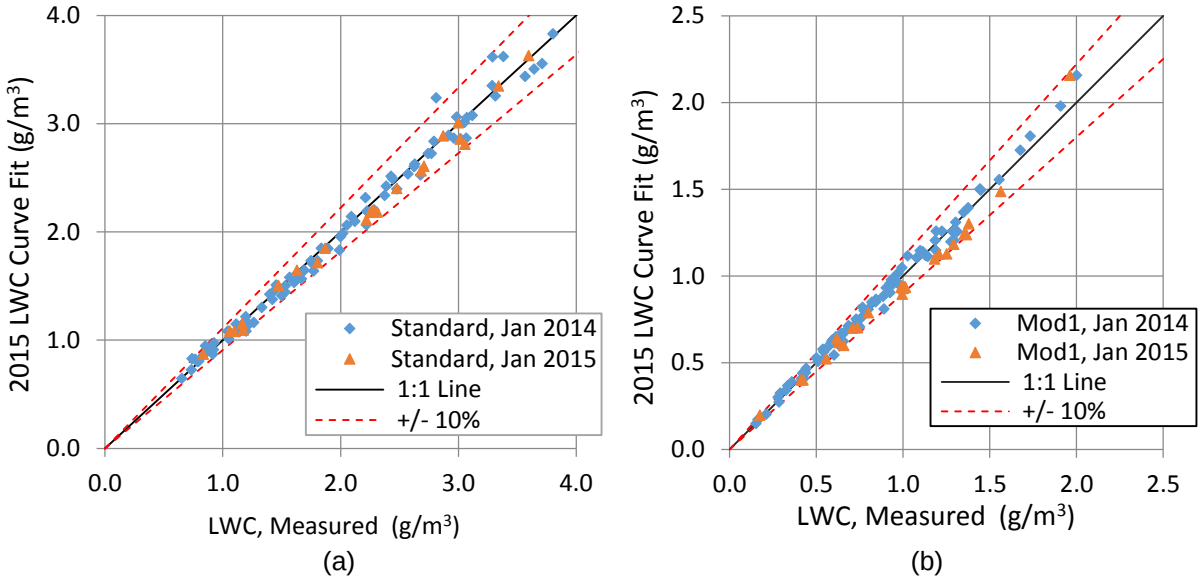

Figure 17.—A comparison of the 2015 curve fits versus measured LWC for (a) Standard nozzles and (b) Mod1 nozzles. The measured LWC data plotted here have been corrected with the three-dimensional collection efficiency.

Correspondingly, the 2015 Mod1 LWC equation is as follows:

$$LWC_{Mod1} = (a * V + b * Pair + c) * \left(\frac{MVD - 2}{d}\right)^{e} * \frac{\sqrt{DeltaP}}{V}$$

Where a = 0.327, b = –0.0591, c = 10.27, d = 23, and e = 0.15, and there is an additional correction factor added to the MVD term to improve the fit. The goodness of fit for this equation is shown in Figure 17(b), which plots the predicted curve fit values against the measured values.

The LWC curve fit equations for large-drop conditions were determined by inputting the measured Pair, DeltaP and LWC into the curve fit generator TableCurve (Systat Software, Inc.). Because of the parameter limitations of the software, one curve was created for the basis velocity value, and then a velocity correction was applied so the equation would account for the velocity dependency of LWC. The collection-efficiency-corrected LWC values for these large-drop conditions remained about the same, because the collection-efficiency correction values did not change significantly for large drop sizes. Figure 18 shows the comparison between the new data and the old (2014) curve fit. Since the data are still largely within 10 percent of the calculated values, it was determined that no further adjustments were necessary for the LWC curve fit in large-drop conditions.

Thus, the LWC curve fit for large-drop conditions is the same as in 2014:

$$LWC_{LD} = \left(a + \frac{b}{Pair} + c * DeltaP + \frac{d}{Pair^2} + e * DeltaP^2 + f * \frac{DeltaP}{Pair} + \frac{g}{Pair^3} + h * \frac{DeltaP^2}{Pair} + i * \frac{DeltaP}{Pair^2}\right) * \left(\frac{V}{k}\right)^{m} \quad (8)$$

where a = 0.1871, b = -0.2469, c = 0.00173, d = –0.0396, e = 0.000107, f = 0.1058, g = 0.6597, h = –0.000713, i = –0.0830, k = 148, and m = –0.75.

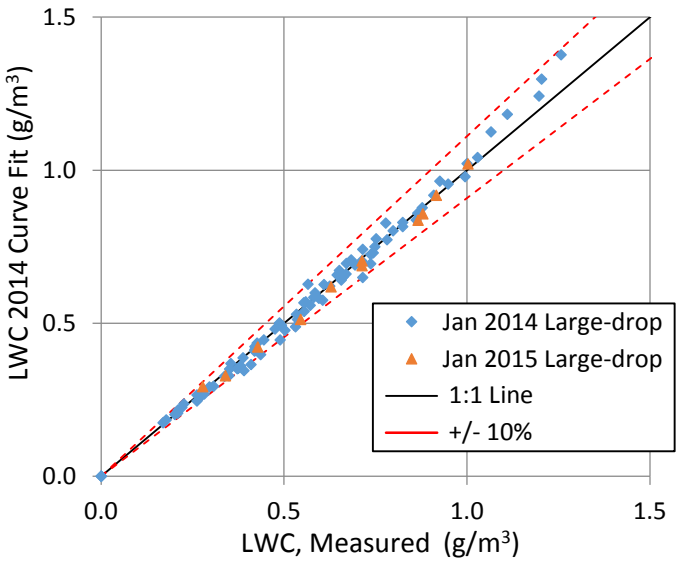

Figure 18.—A comparison of the 2014 curve fit versus measured LWC for all measured large-drop conditions in Jan. 2014 and Jan. 2015. The measured LWC data plotted here have been corrected with the three-dimensional collection efficiency.

Figure 17 and Figure 18 show that the curve fits agree with the majority of the data within 10 percent, even for large-drop conditions, which have a target accuracy of 20 percent.

Operating Envelopes

The IRT's updated 2015 icing envelopes for both the Mod1 and Standard nozzles are compared to the FAA Appendix C icing criteria in Figure 19. The airspeed of 225 kn is selected. At lower air speeds, the curves shift up to higher LWC, at higher air speeds they shift down. While the commonly requested data points MVD = 20 μm, LWC = 0.5 and 1 g/m^3 are easily achieved, another requested point, MVD = 40 μm, LWC = 0.07 g/m^3 will likely never be achieved with the current nozzle design. The 2015 operating envelopes for the large-drop conditions are shown in Figure 20, extending to a maximum MVD of 270 μm. The maximum and minimum calibrated velocities are plotted. Also indicated are the range of temperature-dependent maximum LWC values for each freezing drizzle environmental condition of Appendix O (per Figures 1 and 4 of Ref. 4). Note also that the freezing drizzle (FZDZ) MVD ≤ 40 μm case shown in Figure 20 can be met under Mod1- and Standard-nozzle operating conditions (Figure 19) in the IRT for certain velocities.

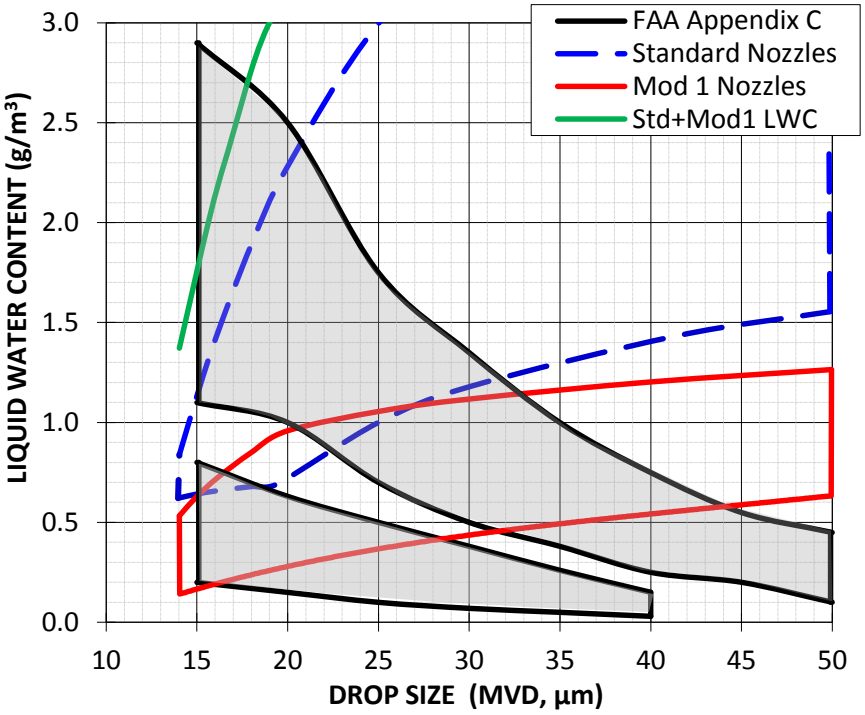

Figure 19.—Comparison of the IRT operating envelopes, LWC versus MVD, to the FAA Icing Certification Criteria for an airspeed of 225 kn. The FAA Appendix C envelopes are shaded and indicated in black. The Mod1 nozzles are in red and the Standard nozzles are in dashed blue. The Mod1 and Standard nozzles can be combined under limited circumstances to produce higher LWC, shown in green.

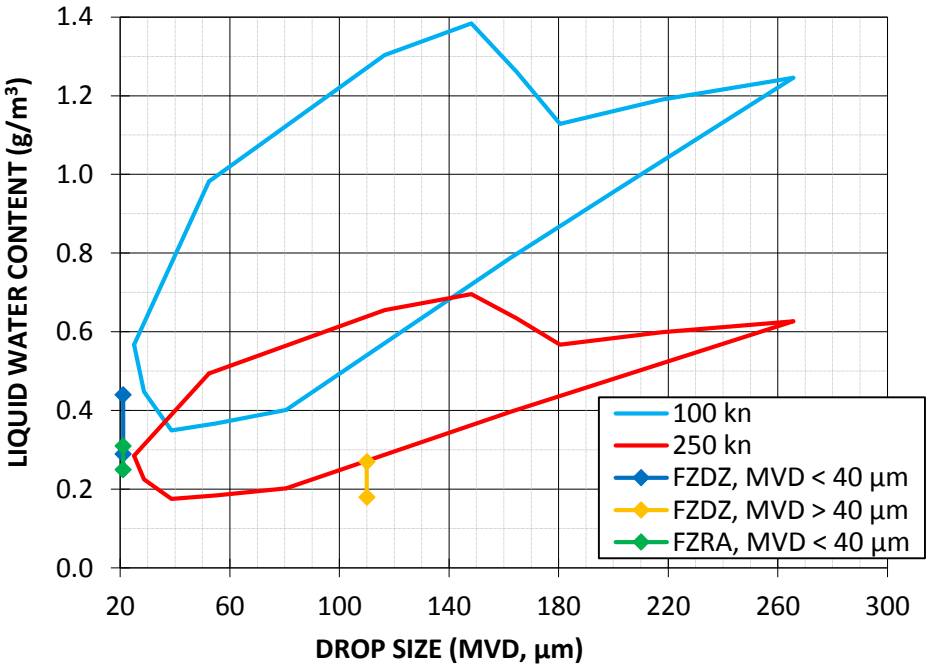

Figure 20.—The IRT large-drop operating envelopes at V = 100 and 250 kn. For reference, the Appendix O max LWC ranges are also shown for each FZDZ and FZRA condition, per figures in Ref. 4. FZRA, MVD > 40 µm has an MVD of 526 µm and an LWC between 0.21 and 0.26 g/m^3, and it is not included on this plot.

Conclusions

The current status of the icing cloud in NASA Glenn's Icing Research Tunnel has been described by outlining the procedures and results of cloud uniformity, liquid water content, and drop-sizing measurements made during the full calibration in January–February 2014 and the interim calibration in January 2015. Overall, the repeatability of cloud uniformity, liquid water content, and median volumetric diameter complied with the requirements laid out in ARP 5905 (Ref. 1).

The 2014 calibration followed the installation of a new set of Mod1 nozzles that had a tighter range of water flow coefficients. The following cloud characteristics were established in January 2014 and are still being used:

- Uniform icing clouds were established with both the Standard and Mod1 nozzles. Cloud uniformity is at ±10 percent for the central region of the test section.
- Calibration equations were established for Standard- and Mod1-nozzle drop size as well as for large-drop liquid water content. The January 2015 interim calibration confirmed that these calibration equations still match the measured data within 10 percent, and no updates were necessary.

In addition, the interim cloud calibration of the IRT was successfully completed in January 2015. There were three main updates that came from the results of this interim calibration:

- There is a high/low spot in the north upper quadrant of the cloud uniformity that has existed since work was done on the spraybars in August 2014. The affected region is more than 18 in. north of centerline. Thorough analysis by the engineers and technicians has not found what caused this region to appear. Since this non-uniformity is in a non-critical region, it will be addressed when schedule allows.
- The MVD calibration curves have been updated for large-drop conditions due to successful operation of the OAP-230Y. The maximum calibrated MVD that can be created in the IRT is now approximately 270 μm. The curve fit equation that was created for large-drop conditions matches the measured values within ±20 percent.
- The LWC calibration curves have been updated for Standard- and Mod1-nozzle operating conditions for MVDs less than 50 μm. This is due to recent work that updated the collection efficiency correction values for the SEA multi-element sensor based on a three-dimensional model of the probe, using particle-size distributions measured in the IRT (Refs. 9 and 10). The updated IRT LWC values are between 1 and 10 percent higher than reported previously.

References

1. SAE ARP-5905, "Calibration and Acceptance of Icing Wind Tunnels," Society of Automotive Engineers. 2009.
2. Van Zante, J. F., Ide, R. F., and Steen, L. E., "NASA Glenn Icing Research Tunnel: 2014 Cloud Calibration Procedure and Results," NASA/TM—2014-218392, October 2014.
3. CFR 14, Part 25, Appendix C, "Atmospheric Icing Conditions," http://www.ecfr.gov/cgi-bin/text-idx?SID=7d39ca0ef6cfde5cc41e26db281fe24d&node=pt14.1.25&rgn=div5#ap14.1.25_11801.c accessed on 3/4/2015, updated annually.
4. CFR 14, Part 25, Appendix O, "Supercooled Large Drop Icing Conditions," http://www.ecfr.gov/cgi-bin/text-idx?SID=7d39ca0ef6cfde5cc41e26db281fe24d&node=pt14.1.25&rgn=div5#ap14.1.25_11801.o accessed on 3/4/2015, updated annually.

5. Ide, Robert. F., Sheldon, David W., "2006 Icing Cloud Calibration of the NASA Glenn Icing Research Tunnel", NASA/TM-2008-215177, May 2008.
6. Miller, Dean R., Addy, Harold E., Ide, Robert F., "A Study of Large Droplet Ice Accretions in the NASA Glenn IRT at Near-Freezing Conditions," NASA/TM—1996-107142/REV1, ARL–MR–294, AIAA–96–0934, June 2005.
7. Science Engineering Associates, "WCM-2000 Users Guide," http://www.scieng.com/ Oct 6, 2010.
8. Frost, W., "Two-dimensional Particle Trajectory Computer Program," Interim Report for Contract NAS3-22448, Mar. 1982.
9. Rigby, D.L., Struk, P.M., and Bidwell, C., "Simulation of Fluid Flow and Collection Efficiency for an SEA Multi-Element Probe," *6th AIAA Atmospheric and Space Environments Conference*, AIAA-2014-2752, 2014.
10. Struk, P.M., NASA Glenn Research Center, personal communication.